# Electronic Supporting information

# A two-year water-stable 2D MOF with aqueous NIR photothermal conversion ability

*Xiang Xue, Jinghang Wang, Qinyi Zhu, Yu Xue and Hewen Liu**

CAS Key Laboratory of Soft Matter Chemistry, Department of Polymer Science and Engineering, University of Science and Technology of China, Hefei, Anhui, 230026, China. E-mail: lhewen@ustc.edu.cn.

**Synthesis of HKUST-1**

HKUST-1 was synthesized according to a process reported by Xiao et al.[1] To a solution of 1,3,5-benzenetricarboxylic acid (0.42 g, 2 mmol) in ethanol (10 mL), the solution of copper acetate monohydrate (0.60 g, 3 mmol) in distilled water (10 mL) was charged under vigorously stirring. Gel-like dark turquoise suspension was obtained. The raw product was then collected by centrifugation at 8000 rpm and washed with ethanol/water (1:1 v/v). The product was divided into two parts. One was redispersed in $H_2O$ for sequential photothermal tests. The other was dried at 120 ºC under reduced pressure for 1 day. The structure of HKUST-1 was verified by using XRD.

**Chemical structure analysis of CuCP-MOF**

The chemical structure of CuCP-MOF was investigated with XPS and FTIR. The Cu nodes inside CuCP-MOF are divalent Cu(II) ions because that the Cu2p XPS shows the well-known shake-up satellites, which are an indication of the presence of Cu(II) species (Fig. S3).[2] As derived from the XPS spectra, the atom ratio of O/Cu was about 5:1 in CuCP-MOF including DMF ligands. Figure S4 compares the FTIR spectra of CPDA ligand, dry CuCP-MOF and activated CuCP-MOF. FTIR spectra show that all the carbonyl group in CuCP-MOFs are complexed in the frameworks. The splitting differences ($\Delta\upsilon$) between the asymmetric (1610 $cm^{-1}$) and symmetric (1420 $cm^{-1}$) carboxylate stretching vibrations are 190 $cm^{-1}$ within the range of 160−200 $cm^{-1}$, elucidating that the carboxylate group in CuCP-MOF is bridging bidentate,[3] as in zinc

and copper paddlewheel structures.[4, 5] The peak at 1660 $cm^{-1}$ in dry CuCP-MOF (pointed with an arrow in Fig. S4) arises from DMF ligands, which disappears in the activated CuCP-MOF.

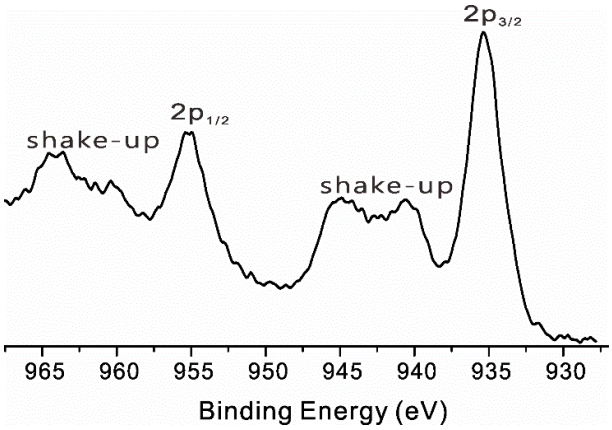


**Fig. S1** Cu2p XPS of CuCP-MOF.

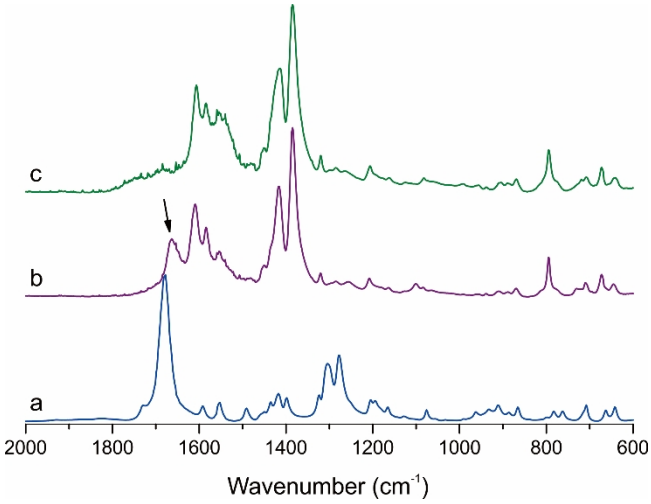


**Fig. S2** FTIR of CuCP-MOF and ligand CPDA. (a) Ligand CPDA. (b) Dry CuCP-MOF. (c) Activated CuCP-MOF without DMF ligands. The arrow pointed is from the vibration of DMF.

**Synthesis and structure determination of single crystals of CuCP-MOF**

Single crystalline CuCP-MOF samples synthesized from copper(II) nitrate trihydrate were prepared for the analysis of crystalline structure. To obtained larger size single crystals suitable for single crystal analysis, modulated synthesis of CuCP-MOF was performed, using acetic acid (AA) as the modulator. Experimental details of modulated synthesis of CuCP-MOF are listed in Table S1. Three parallel experiments AA-1, AA-2 and AA-3 are performed. The size of CuCP-MOF crystals can be significantly increased by adding acetic acid, observed under an optical microscope (Fig. S1). In addition, elongated reaction time can also increase the size of crystals. The lateral size of crystals reaches ca. 0.15 cm in 20 days (AA-3) (Fig. S1d).

**Table S1.** Experimental details of modulated synthesis of CuCP-MOF.

| | AA-1 | AA-2 | AA-3 |
|---|---|---|---|
| acetic acid (μL) | 138 | 386 | 386 |
| CPDA (mg) | 24 | 24 | 24 |
| $Cu_2(NO_3)_2•3H_2O$ (mg) | 20 | 20 | 20 |
| DMF (mL) | 3 | 3 | 3 |
| Temperature (℃) | 80 | 80 | 80 |
| Reaction time (d) | 5 | 7 | 20 |

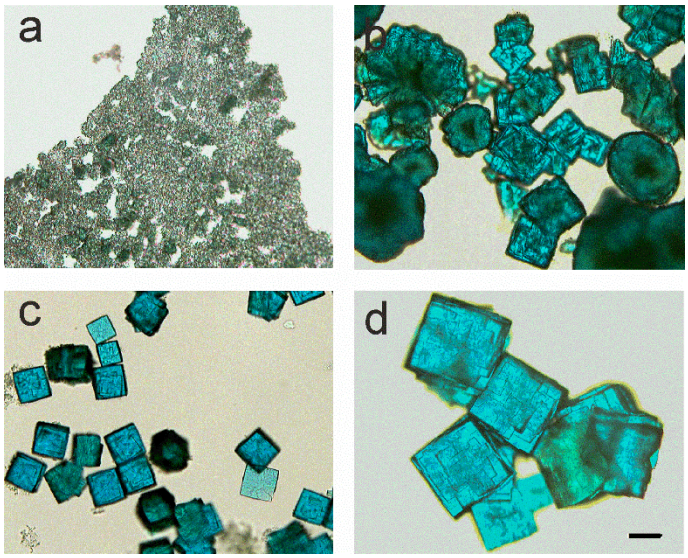


**Fig. S3** Optical micrograph images of CuCP-MOFs obtained from the solution reaction method. Optical micrograph images of (a) CuCP-MOFs prepared without acetic acid, (b) AA-1, (c) AA-2 and (d) AA-3. The scale bar is 50 μm.

**Table S2**. Crystal Data and simulated structure of CuCP-MOF.

| | Measured | DFT Simulated |
|---|---|---|
| formula | $Cu(C_{18}H_{14}O_4)\cdot DMF$ | |
| M (g/mol) | 378.86 | |
| symmetry | triclinic | |
| space group | P -1 | |
| a (Å) | 10.0650(3) | 10.2201 |
| b (Å) | 10.8974(15) | 11.2676 |
| c (Å) | 10.9395(15) | 11.2380 |
| α (deg) | 90.676(11) | 90.788 |
| β (deg) | 91.729(16) | 91.243 |
| γ (deg) | 92.725(16) | 93.776 |
| V ($Å^3$) | 1197.9(4) | 1290.9 |
| Z | 2 | 2 |
| density ($g/cm^3$) | 1.0358 | |
| reflns collected | 10554 | n.a. |
| unique reflns ($R_{int}$) | 4076 (0.1041) | n.a. |
| $R_1$, $wR_2$ | 0.1397, 0.3617 | n.a. |
| CCDC numbers | 1992673 | 2016757 |

About Alert A (Ratio Observed / Unique Reflections (too) Low): Though 23178 valid reflections were recorded from a single crystalline sample by the single crystal

diffractometer in several runs, 6890 reflections were used for space-group determination, and only 2319 reflections were used for UB fit.

We have also tried to get single crystalline diffractions in a Mo K-alpha X-ray diffractometer (Bruker D8 Venture single crystal diffractometer with Mo Kα radiation (λ = 0.71073 Å), Shanghai Institute of Materia Medica, Chinese Academy of Sciences). However, we could not get any better diffractions. Therefore we attributed the issue of Low Ratio Observed / Unique Reflections to the layer structure with weak interlayer interactions. The easy delaminated layer structure and many disordered solvent molecules were the main reasons causing many rejected reflections. The disorder of DMF coordination is one of the reasons causing not good results of $R_1$ and $wR_2$ listed in Table S2.

About Alert A (VERY LARGE Solvent Accessible VOID(S) in Structure): There are many not identified solvent molecules (DMF) in the single crystals.

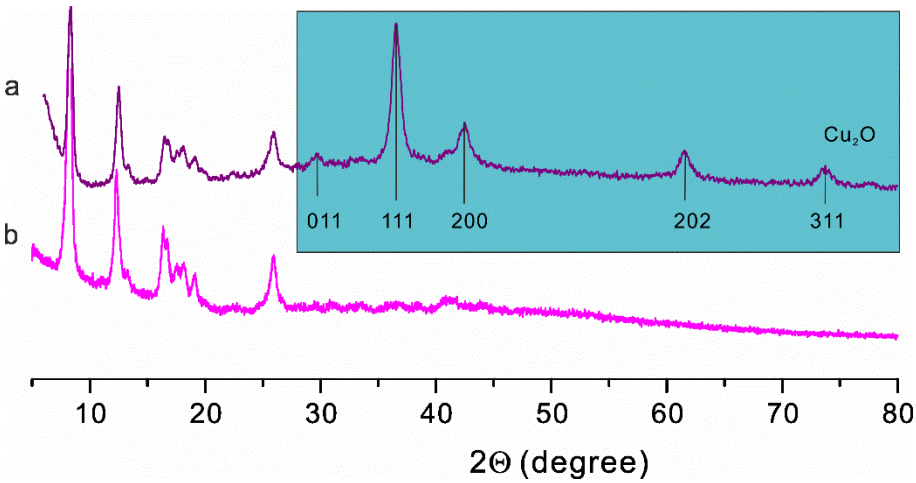


**Fig. S4** XRD patterns of CuCP-MOF synthesized in air (a) or in an inert atmosphere (b). The peaks inside a frame in (a) arise from $Cu_2O$ in cubic pn3m phase (JCPDS No. 65-3288).

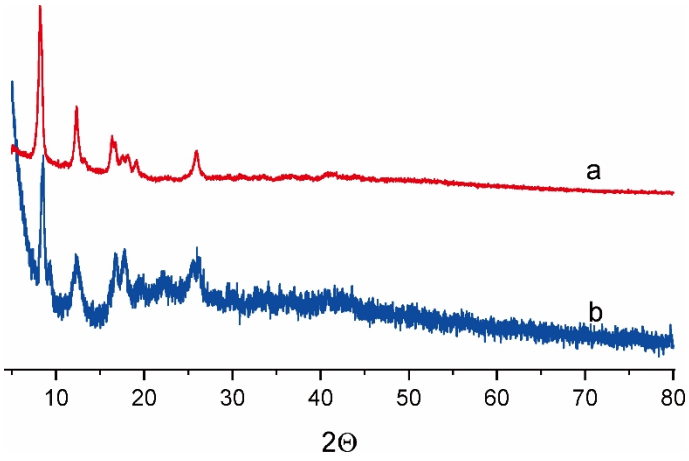


**Fig. S5** XRD of CuCP-MOF obtained from cupric nitrate (a) or cupric acetate (b). Because of the thinner film samples, the XRD peaks of CuCP-MOF synthesized from cupric acetate are broader than those of CuCP-MOF prepared from cupric nitrate.

**Table S3.** Average bond lengths (Å) in the paddlewheel structure of CuCP-MOF.

| | measured | DFT-simulated |
|---|---|---|
| Cu1-Cu2 | 2.562 | 2.5415 |
| Cu1-O1 | 1.985 | 1.9614 |
| C1-O1 | 1.214 | 1.2690 |
| C1-C2 | 1.528 | 1.4944 |
| O5-Cu1 | 2.391 | 2.2104 |

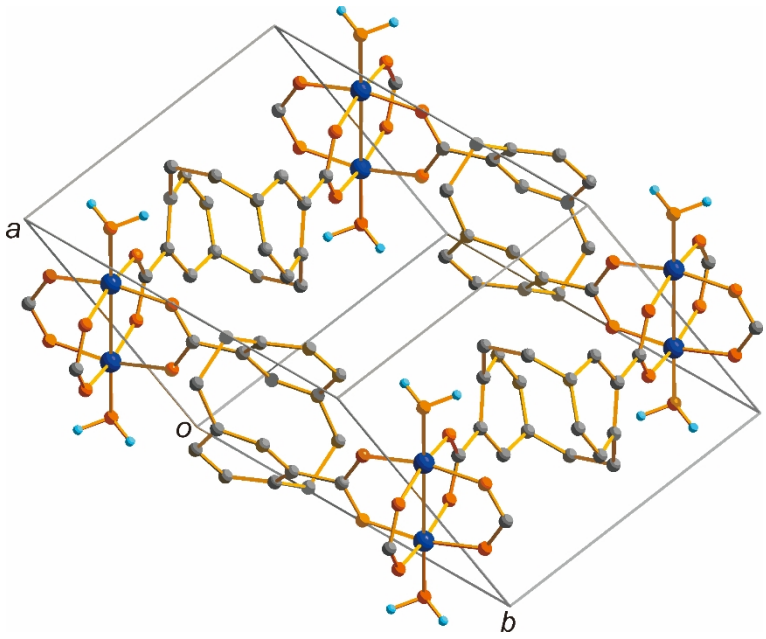


**Fig. S6** A simulated structure of CuCP-MOF with apical water ligands. The resultant skew cell is a triclinic cell ($a$ = 9.1748 Å, $b$ = 10.8330 Å, $c$ = 10.9841 Å, α = 86.6138°, β = 111.4117°, γ = 119.8250°).

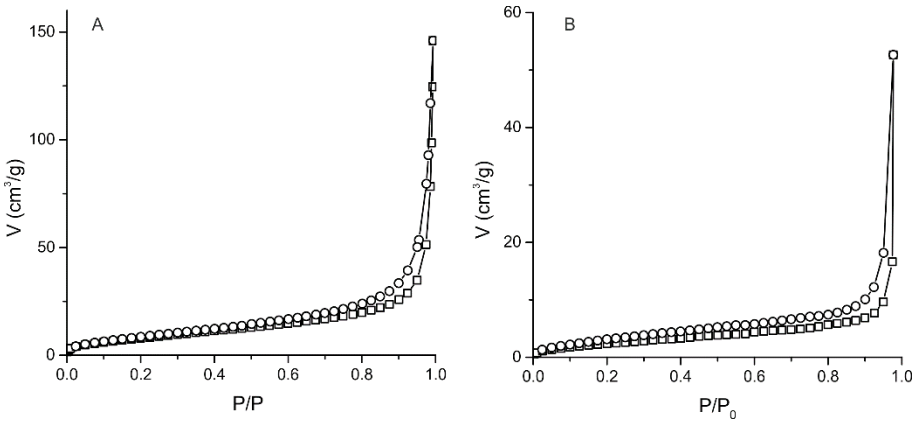


**Fig. S7** $N_2$ adsorption and desorption isotherms of CuCP-MOF at 77 K. (A) Dry CuCP-MOF sample. (B) CuCP-MOF sample activated at 250 °C to remove DMF ligands.

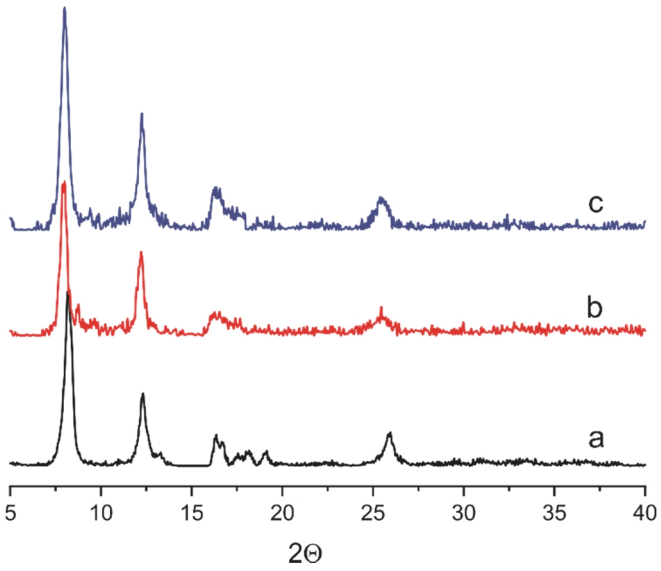


**Fig. S8** XRD of CuCP-MOFs after being dispersed in water with different pH values for three days. (a) Pristine CuCP-MOF, (b) pH = 8, (c) pH = 3.2.

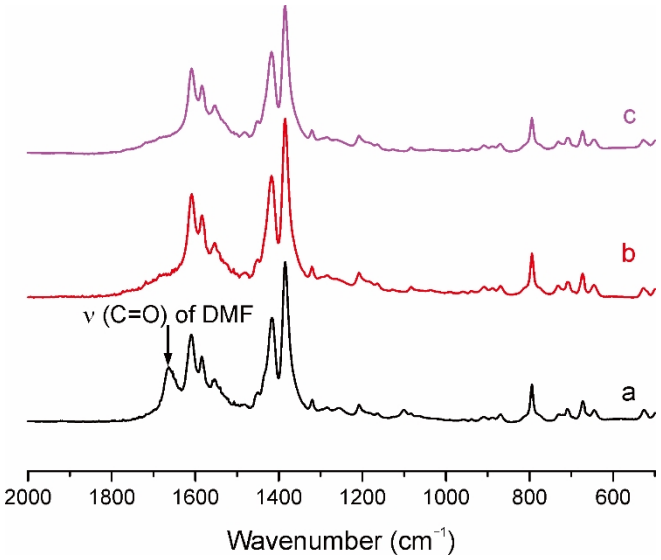


**Fig. S9** FTIR of CuCP-MOFs after being dispersed in water with different pH values for three days. (a) Pristine CuCP-MOF, (b) pH = 3.2, (c) pH = 8.

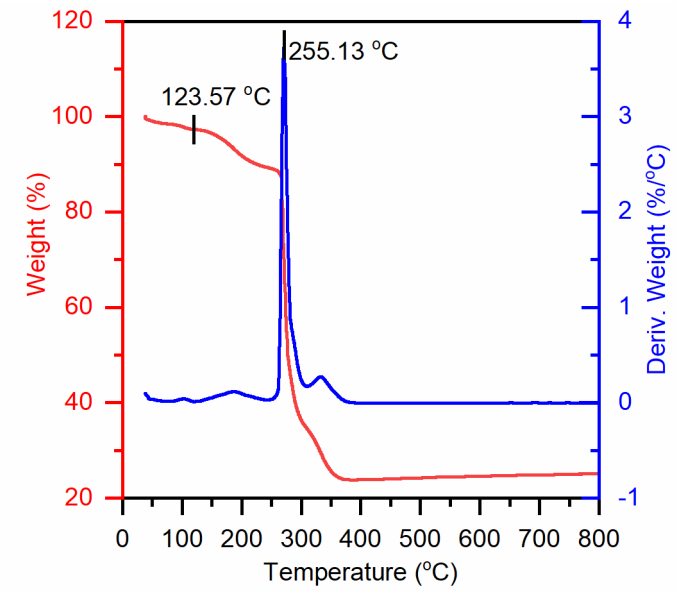


**Fig. S10** Differential thermal analysis of CuCP-MOF, which shows that the detachment of DMF ligands of CuCP-MOF starts at about 124 ℃.

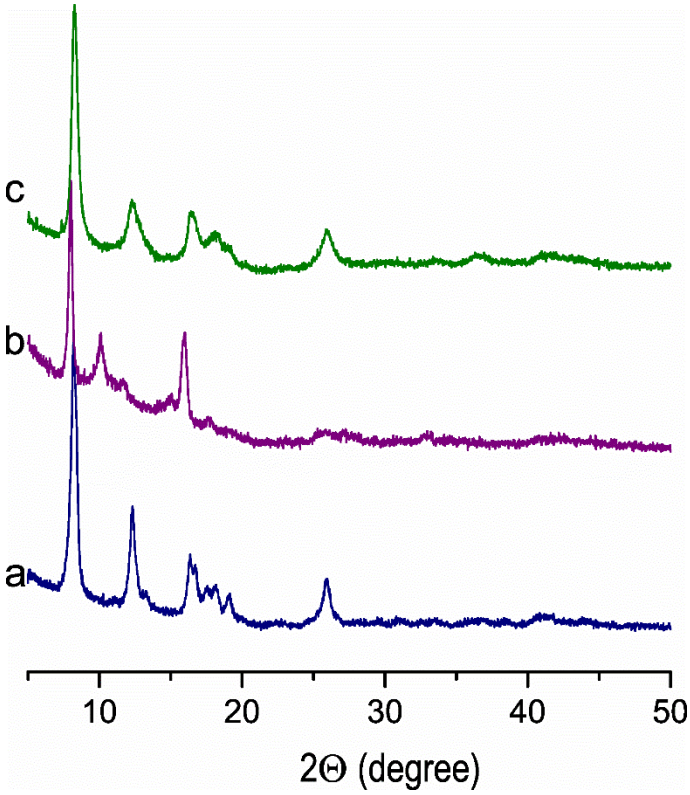


**Fig. S11** XRD patterns of CuCP-MOF in reversible solvent ligand tests. (a) Dry samples. (b) Activated sample. (c) Recovered sample from activated CuCP-MOF by mixing the activated sample with DMF.

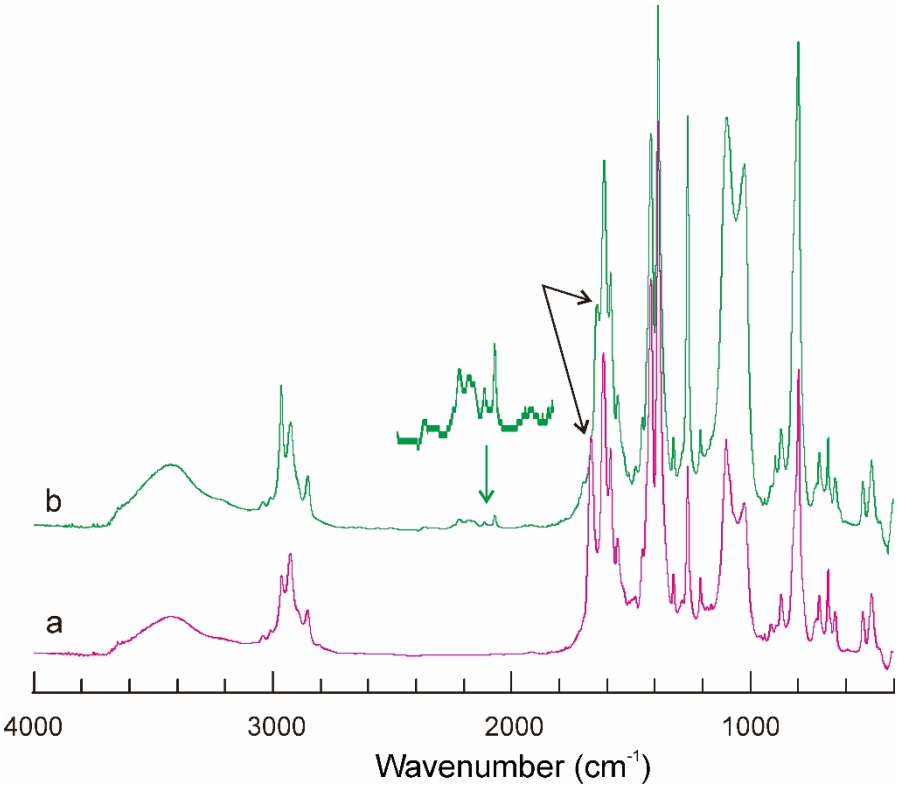


**Fig. S12** FTIR of CuCP-MOF after ligand exchange with DMF-*d*7. (a) Pristine sample. (b) CuCP-MOF dispersed in DMF-*d*7 for three days. The inset of b is from the vibrations of DMF-d6.

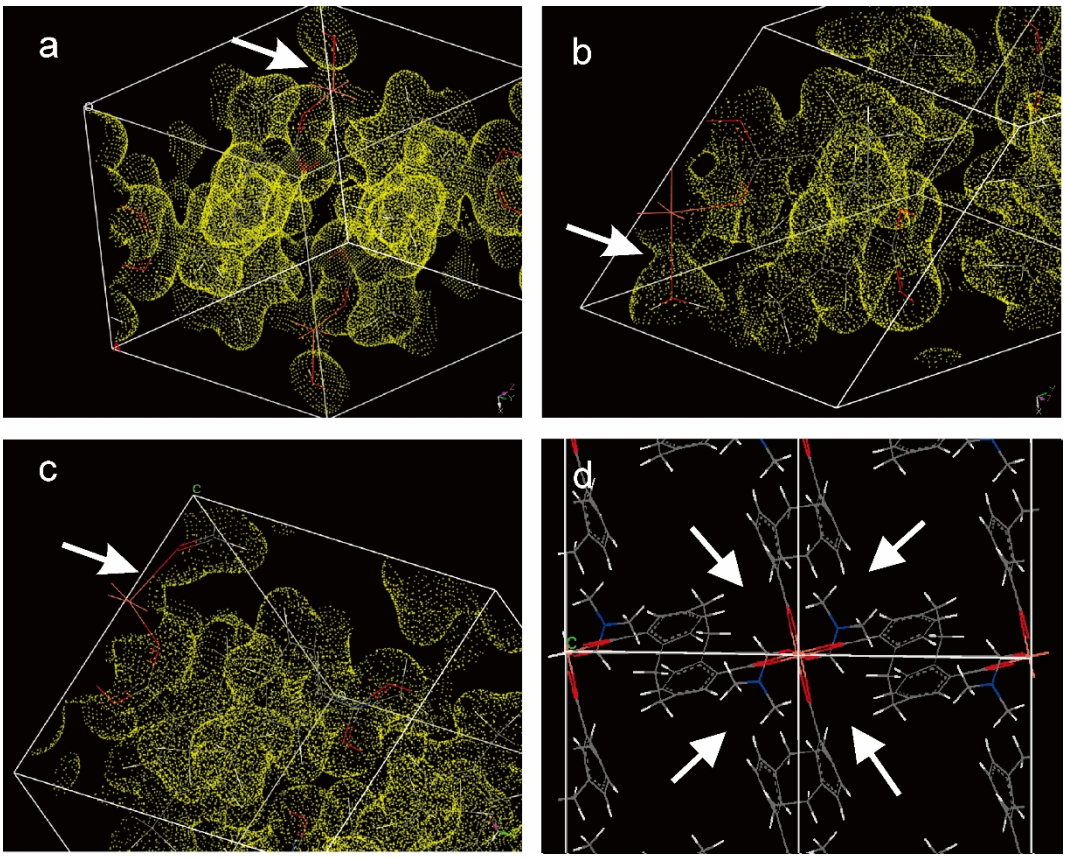


**Fig. S13** Factors affecting the water stability of CuCP-MOF. (a-c) The total electron densities of the DFT-optimized structures of (a) fixed CuCP-MOF structure with apical water ligands, (b) the fully relaxed structure with apical water ligands and (c) CuCP-MOF with apical DMF ligands. (d) The PW structure is sheltered by 3D CPDA liands.

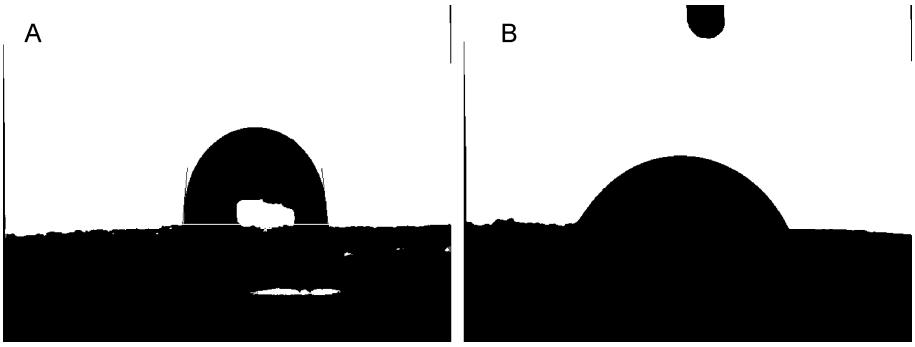


**Fig. S14** Water contact angles of CuCP-MOF and HKUST-1. (A) CuCP-MOF. (B) HKUST-1. Fine MOF powders are pressed into disks under a pressure of 10 MPa for water contact angle measurements.

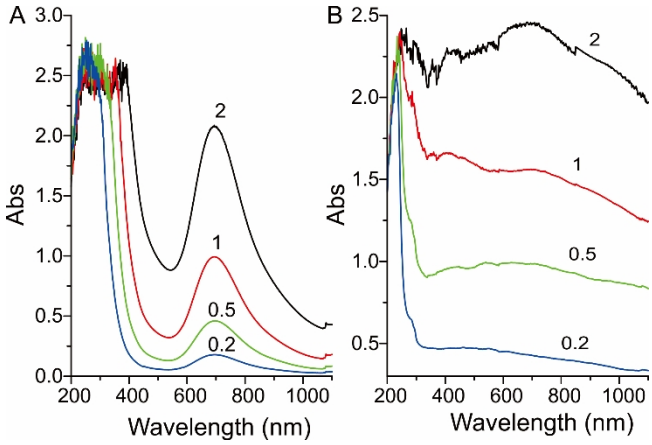


**Fig. S15** UV-vis-NIR absorption spectra of the aqueous dispersions of CuCP-MOF and HKUST-1 at different concentrations. (A) CuCP-MOF. (B) HKUST-1. The values above the curves are the concentrations (mg/mL).

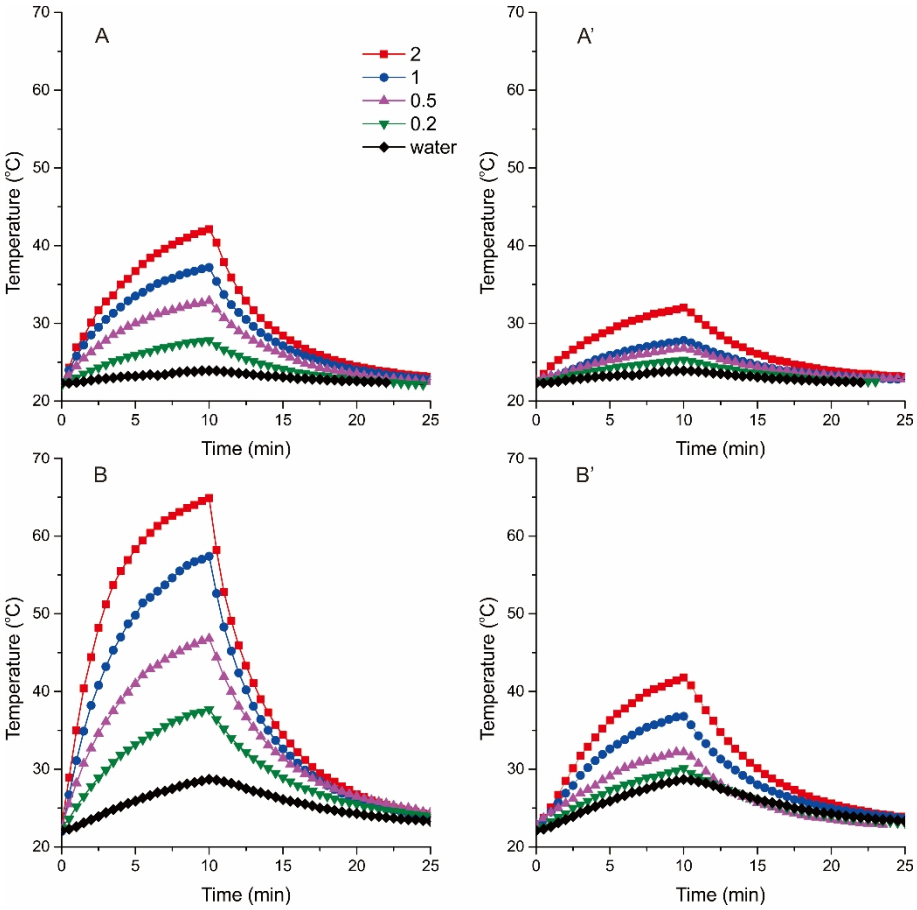


**Fig. S16** NIR-thermal conversion by aqueous dispersions of CuCP-MOF or HKUST-1 under irradiation of 808 nm laser. The data include two parts: temperature elevation by laser irradiation in 10 minutes and successive natural cooling after turning off laser. (A, B) CuCP-MOF. (A′, B′) HKUST-1. The power density of laser is 2.0 W/cm$^2$ (A, A′) or 5 W/cm$^2$ (B, B′). The same legends in (A) indicating the corresponding concentrations (mg/mL) for all panels.

**Table S4**. NIR (808 nm) photothermal conversion efficiency of CuCP-MOF and HKUST-1 in water

| C (mg/mL) | $\eta_C$ (%)[a] | $\eta_H$ (%)[a] | $\eta_C$ (%)[b] | $\eta_H$ (%)[b] |
|---|---|---|---|---|
| 2 | 18.5 | 5.7 | 21.9 | 7.6 |
| 1 | 19.4 | 3.5 | 20.1 | 3.5 |
| 0.5 | 16 | 2.9 | 22.5 | 2.5 |
| 0.2 | 16.2 | 1.3 | 23.5 | 2.2 |

[a] NIR photothermal conversion efficiency $\eta_C$ of CuCP-MOF and $\eta_H$ of HKUST-1. The power density of laser is [a] 5 W/cm$^2$ and [b] 2 W/cm$^2$.

REFERENCES

1. Xiao, B.; Yuan, Q.; Williams, R. A. Exceptional function of nanoporous metal organic framework particles in emulsion stabilisation. *Chem. Commun.* **2013,** 49, 8208-8210.

2. Biesinger, M. C.; Lau, L. W. M.; Gerson, A. R.; Smart, R. S. C. Resolving surface chemical states in XPS analysis of first row transition metals, oxides and hydroxides: Sc, Ti, V, Cu and Zn. *Appl. Surf. Sci.* **2010,** 257, 887-898.

3. Parikh, S. J.; Mukome, F. N. D.; Zhang, X. M. ATR-FTIR spectroscopic evidence for biomolecular phosphorus and carboxyl groups facilitating bacterial adhesion to iron oxides. *Colloids Surf. B* **2014,** 119, 38-46.

4. Li, H.; Eddaoudi, M.; Groy, T. L.; Yaghi, O. M. Establishing microporosity in open metal-organic frameworks: Gas sorption isotherms for Zn(BDC) (BDC = 1,4-benzenedicarboxylate). *J. Am. Chem. Soc.* **1998,** 120, 8571-8572.

5. Carson, C. G.; Hardcastle, K.; Schwartz, J.; Liu, X. T.; Hoffmann, C.; Gerhardt, R. A.; Tannenbaum, R. Synthesis and Structure Characterization of Copper Terephthalate Metal-Organic Frameworks. *Eur. J. Inorg. Chem.* **2009**, 2338-2343.